View metadata, citation and similar papers at core.ac.uk
brought to you by CORE
provided by NASA Technical Reports Server

N95-11059

UV-B RADIATION AMPLIFICATION FACTOR DETERMINED BASED ON THE SIMULTANEOUS OBSERVATION OF TOTAL OZONE AND GLOBAL SPECTRAL IRRADIANCE

T. ITO, Y. SAKODA, and K. MATSUBARA,
Observations Department, Japan Meteorological Agency
1-3-4 Otemach, Chiyodaku, Tokyo 100. JAPAN

R. KAJIHARA, T. UEKUBO, M. KOBAYASHI, M. SHITAMICHI, T. UENO and M. ITO
Aerological Observatory
1-2 Nagamine, Tsukuba, Ibaraki 305. JAPAN

ABSTRACT

The Japan Meteorological Agency started the spectral observation of solar ultraviolet (UV) irradiance on 1 January 1990 at Tateno, Aerological Observatory in Tsukuba (36°N, 140°E). The observation has been carried out using the Brewer spectrophotometer for the wavelengths from 290 to 325 nm with a 0.5 nm interval every hour from 30 minutes before sunrise to 30 minutes after sunset throughout a year. Because of remarkable similarity within observed spectra, an observed spectrum can be expressed by a simple combination of a reference spectrum and two parameters expressing the deformation of the observed spectrum from the reference. By use of the relation between one of the deformation parameters and the total ozone simultaneously observed with the Dobson spectrophotometer, the possible increase of UV irradiance due to ozone depletion is estimated. For damaging UV (DUV; Wester,1981), the irradiance possibly increases about 19% with the ozone depletion of 10% at noon throughout the year in the northern mid-latitudes. DUV at noon on the summer solstice possibly increases about 5.6% with the ozone depletion of 10 m atm-cm for all latitudes in the Northern Hemisphere.

1. INTRODUCTION

The possible adverse effects of solar ultraviolet (UV) irradiance increase due to ozone depletion have become of great concern in the world. Theoretical studies of UV increase due to ozone depletion have been made extensively since the 1970's (for example, Cutchis, 1974; Venkateswaran, 1974; Dave and Halpern, 1976; Pyle and Derwent, 1980; Gelstl et al., 1981), whereas the studies based on observed UV data have not been made enough so far.

The Japan Meteorological Agency (JMA) started the spectral observation of global irradiance of solar ultraviolet (UV) on 1 January 1990 at Tateno, Aerological Observatory in Tsukuba (36.05 N, 140.00 E). The observations were also started at Sapporo, Kagoshima and Naha on 1 January 1991, and at Syowa Station, Antarctica, on 1 February 1991. This paper aims to explain the result of the analyses of observations in Tsukuba in 1990, focusing on the assessment of the possible UV increase due to ozone depletion. The details of the entire work have been published in Japanese (Ito et al., 1991).

2. OBSERVATION

The instruments used in the JMA network are the Brewer spectrophotometer improved on the old version used by Josefsson (1986). The important improvements are: (1) The polarization prism is substituted by the film polarizer placed on the filter wheel, so that the polarizer is only used for ozone observations and not for UV spectral observation. (2) The width of the spectral scan is extended to 290 - 325 nm from the old version's 290 - 320 nm. (3) The software of the Brewer is amended so as to enable the scheduling of daily observation based on local time, instead of solar zenith angle which is used in the old version. (4) The software written with GW-BASIC is translated to that with N88-BASIC to allow using a NEC Personal Computer as a control unit, which enables us to display the observed spectra on the CRT after each observation.

In Tsukuba, the Brewer #52 is installed near the southwest corner of the roof-top of the observatory where nothing bars the view field of the UV port of the Brewer. The UV port is placed 0.9 m above the roof floor, 14 m above the ground and 39 m above the sea level. The Brewer is operated in its automatic continuous operation mode and the observations are made every hour from 30 minutes before sunrise to 30 minutes after sunset every day. The measurement of UV spectra takes about 8 minutes per once, scanning the wavelengths with a 0.5 nm interval, upward from 290 to 325 nm, and then downward from 325 to 290 nm.

The calibration of the Brewer has been conducted at the Observatory against the NBS standard lamp (1000 Watt). From the regular internal and external lamp tests, the responsivity change less than 7% is noted in 1990. The observed spectra are corrected for this change prior to the analyses.

3. ANALYSIS OF OBSERVED SPECTRA

3.1 Parameterization of observed spectra

The observed spectra show remarkable similarities in both the general and fine structures of the spectra. Noting this similarity, an observed spectrum is expressed by a simple combination of a reference spectrum at a given solar zenith angle and two parameters expressing the deformation of the observed spectrum from the reference. The reference spectrum is determined as a function of solar zenith angle, based on the observed spectra in the following procedure.

Figure 1 shows the scatter diagrams of measurements with the Brewer (photon count rate) and solar zenith angles. The data is taken from those for the wavelength channel 305 nm and the period from 1 April to 30 June. The curve along the upper boundary of plotted data is approximated in a form of Eq. 1.

$$\log CR(\lambda, za) = \sum_{i=1}^{n} Q_i(\lambda) \cdot \cos(\pi \cdot (i-1) \cdot za/180) \quad (1),$$

where λ is wavelength; za is solar zenith angle; $CR(\lambda,za)$ is photon count rate; $Q_i(\lambda)(i=1,2,\ldots,8)$ is the coefficient to be determined for each wavelength. Note that a scaling of λ = (L-325)/0.5 is used to convert the wavelength L in nm unit to the nondimensional wavelength λ.

After the determination of $Q_i(\lambda)$ for 71 wavelength channels, the reference UV spectral irradiance $F(\lambda,za)$ is determined by

$$F(\lambda, za) = \frac{CR(\lambda, za) - CR(290, za)}{R(\lambda)} \quad (2),$$

where $R(\lambda)$ is the spectral responsivity of the Brewer #52. The count rate CR(290,za) at the shortest wavelength is assumed as the stray light and used for the stray light correction of the spectral irradiance.

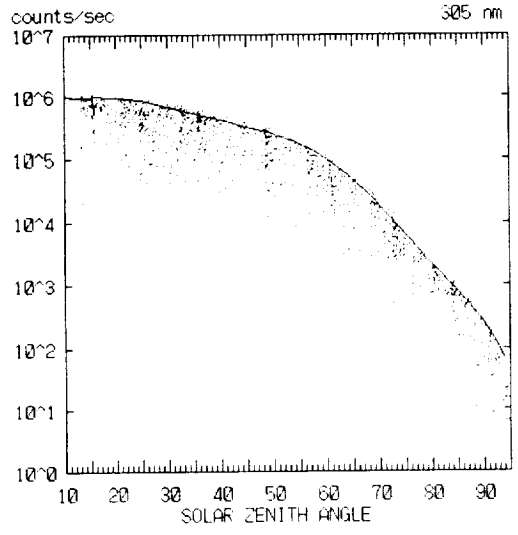

Fig. 1 Scatter diagram of photon count rates plotted against solar zenith angles for the 305 nm wavelength channels of the Brewer, obtained from 1 April to 30 June in 1990.

Figure 2 shows the comparison between the observed (OBS) and reference (REF) spectrum, and the spectral difference (LOR: log(OBS/REF)). The left ordinate indicates the logarithmic scale of spectral irradiance ($\mu W/m^2$ nm), and the right is the scale for LOR.

3.2 Deformation parameter

The general resemblance of fine structures between the OBS and REF spectrum can be seen in Fig. 2, which is well demonstrated by the smoothness of the LOR curve, at least for the wavelengths longer than 300 nm, even though the OBS and REF curve exhibits notable fluctuations in this wavelength region. The irregular fluctuations of the LOR curve at the wavelengths shorter than 295 nm is due to the low irradiance near the detection limit of the Brewer.

Similar resemblance between OBS and REF is seen in almost all observations. Then, the LOR curves are approximated for the wavelength longer than 300 nm by the following quadratic curve:

$$LOR = \alpha\lambda^2 + \beta \quad (3),$$

where α and β are the parameters to be determined with each of the observed spectra.

In Fig. 2, the thick line indicates the quadratic curve thus determined. The fitness of the curves can be evaluated by the standard deviation of the LOR curve around the quadratic curve. In all, 4288 spectra are obtained in 1990 at solar zenith angles ranging from 13 to 90 degree. Among them, 96% of LOR curves are successfully approximated in the form Eq. 3 with the standard deviations less than or equal to 0.06, and 76% are less than or equal to 0.03. The standard deviation of 0.03 corresponds to the deviation of about 7% in irradiance, which is quite small compared to the natural variability.

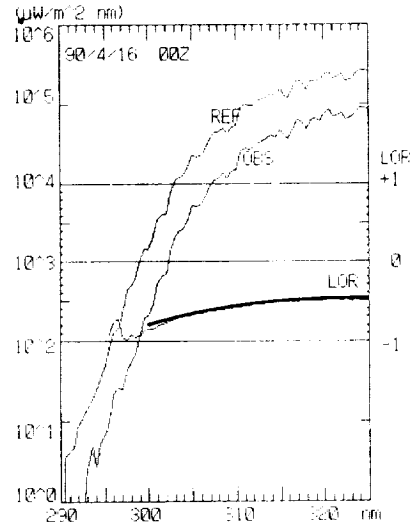

Fig. 2 Comparison between the observed (OBS) and reference (REF) spectra of solar UV irradiance and the logarithmic difference (LOR) between the REF and OBS.

Eventually, an observed UV spectral irradiance is expressed as

$$I(\lambda, za, \tau, oz, al, \cdots) = F(\lambda, za) \cdot 10^{\alpha\lambda^2+\beta} \quad (4),$$

where τ, oz and al are atmospheric optical thickness (the effect of clouds and aerosols), total ozone and ground albedo, respectively. Hereafter, α and β are called the deformation parameters, meaning they express the deformation of an observed spectrum from the reference spectrum of a relevant solar zenith angle. The parameter α indicates the degree of the wavelength-dependent deformation and is expected to correlate mainly with oz. The parameter β indicates the degree of the wavelength-independent deformation and is expected to correlate with τ and al.

3.3 Relation between parameter α and total ozone

The bottom diagram in Fig. 3 shows the time series of total ozone observed with the Dobson spectrophotometer for the period from 1 January to 31 December 1990. The top diagram in Fig. 3 shows the time series of the deformation parameter α at the same time when the total ozone is observed, interpolated with the hourly values. Comparing these two time series in Fig. 3, it can be noticed that the change of α is in good accord with that of total ozone. With careful examination, however, it is realized that the time change of α is perfectly identical in phase to that of total ozone, but it is not the case in amplitude, suggesting that the sensitivity of α to total ozone is not uniform, but depends on solar zenith angle.

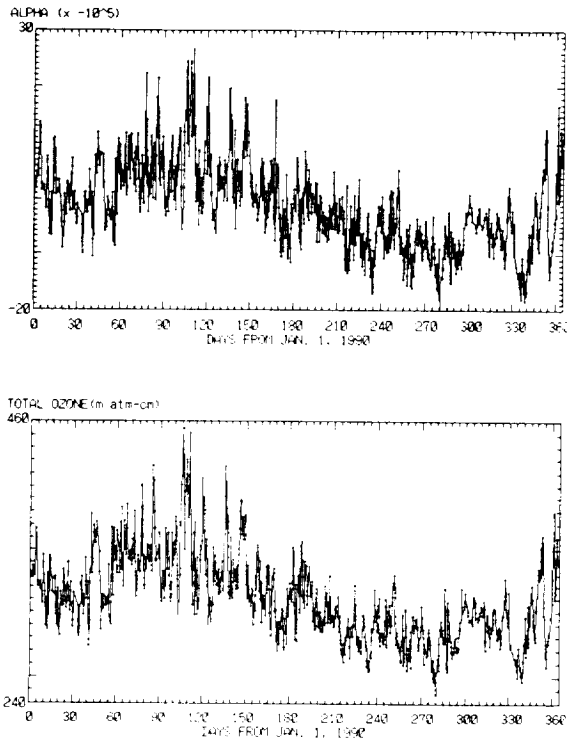

Fig. 3 Comparison of α (top) and total ozone with the Dobson (bottom).

The total ozone is observed at the solar zenith angle between 13° and 70° in Tsukuba. All the simultaneous pairs of total ozone oz and deformation parameter α are classified into six groups based on the solar zenith angle at which the total ozone is observed. Each group is characterized by the different solar zenith angle range with a 10° interval, starting from 10°. Figure 4 shows an example of the scatter diagrams of oz and α for the solar zenith angles from 60° to 70°. The pairs of oz and α in this group amounts to 304 and the correlation coefficient between oz and α is 99.2%. Similar good correlation is seen in all solar zenith angle intervals.

Table 1 shows the mean solar zenith angles, the regression coefficient that is the gradient of the regression line; ($d\alpha/doz$)), the offsets of the regression lines, standard deviations of α (self standard deviations), standard deviations of α from the regression line (regression standard deviations), correlation coefficients, and data amounts, corresponding to each solar zenith angle interval.

3.4 Increase of monochromatic irradiance due to ozone depletion

The logarithmic differentiation to Eq. 4 and the multiplication of each side by 100 will lead to Eq. 5:

$$\frac{100}{I(\lambda)} \cdot \frac{dI(\lambda)}{doz} = 230 \cdot \lambda^2 \cdot \frac{d\alpha}{doz} \quad (5).$$

In this derivation, the dependency of β on oz is ignored by assuming monochromatic irradiance of the maximum wavelength 325 nm is independent on the ozone amount. The left side of this equation

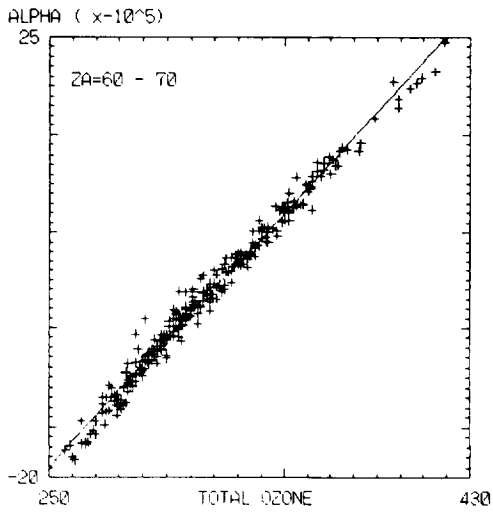

Fig. 4 Scatter diagram of α and total ozone for the zenith angles of 60-70°.

means the percent change of monochromatic UV irradiance due to a 1 m atm-cm change of total ozone. Hereafter we call it RAC (Radiation Amplification Coefficient).

The values of $d\alpha/doz$ are the regression coefficients, listed in Table 1 and plotted in Fig. 5 as a function of solar zenith angle. The curve in Fig. 5 is expressed by

$$d\alpha/doz = const \times (\cos^{m}(za) + \delta)^{-(1+\epsilon)/m} \quad (6),$$

where const = 0.141609, m = 6, δ = 0.029497 and ϵ = 0.0808, which are determined by the least square fitting to the plotted data.

Tab. 1 Correlation between total ozone and deformation parameter α.
ZA: solar zenith angle;
GAR: gradient of regression line;
OFF; offset of regression line;
ST DEV: standard deviation around the average;
DEV REG: standard deviation from the regression line;
COR COEF: correlation coefficient;
NUM: number of data.

ZA	α		ST DEV	DEV REG	COR COEF	NUM
	GRA	OFF				
16.2	-1.44E-6	4.59E-4	4.03E-5	1.10E-5	0.9618	28
25.0	-1.64	5.31	5.65	1.44	0.9671	26
35.2	-1.68	5.74	5.95	1.17	0.9804	24
48.1	-2.03	6.71	6.87	1.08	0.9876	203
55.4	-2.35	7.59	6.78	0.92	0.9908	79
66.9	-2.61	8.43	8.29	1.05	0.9920	308

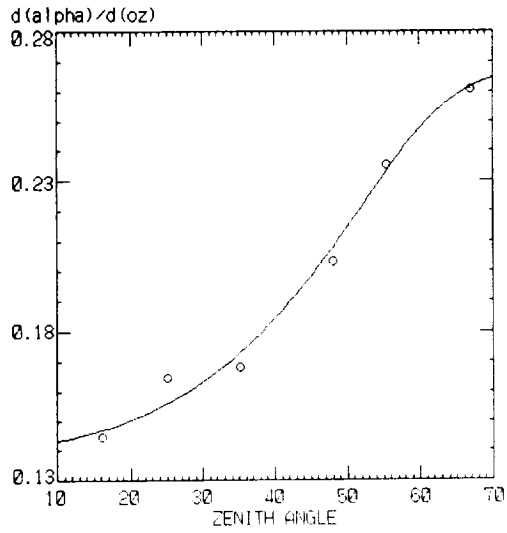

Fig. 5 Plot of the regression coefficients $d\alpha/doz$ against the solar zenith angles za listed in Table 1.

The values of RAC can be calculated with Eqs. 5 and 6 for any solar zenith angle, at least, between 10° and 70°. Figure 6 shows the relationship between RAC and wavelength for several solar zenith angles indicated by the numbers attached to the curves. It should be noted that the values of RAC for the wavelength shorter than 300 nm in Fig. 6 are given as a extrapolation because the values of α are determined based on the observed spectra for the wavelength range from 300 nm to 325 nm.

3.5 Increase of damaging UV due to ozone depletion

Here, DUV (damaging ultraviolet) is defined as the integration of UV spectral irradiance, weighted by the action spectrum formulated by Wester(1981). The expression of RAC for DUV is given by

$$\frac{100}{DUV}\cdot\frac{dDUV}{doz} = 230\cdot\lambda_{av}^{2}\cdot\frac{d\alpha}{doz} \quad (7),$$

$$\lambda_{av}^{2} = \frac{\int_{\lambda_1}^{\lambda_2} D(\lambda)\cdot F(\lambda, za)\cdot 10^{\alpha\lambda^2+\beta}\cdot\lambda^2 d\lambda}{\int_{\lambda_1}^{\lambda_2} D(\lambda)\cdot F(\lambda, za)\cdot 10^{\alpha\lambda^2+\beta} d\lambda} \quad (8),$$

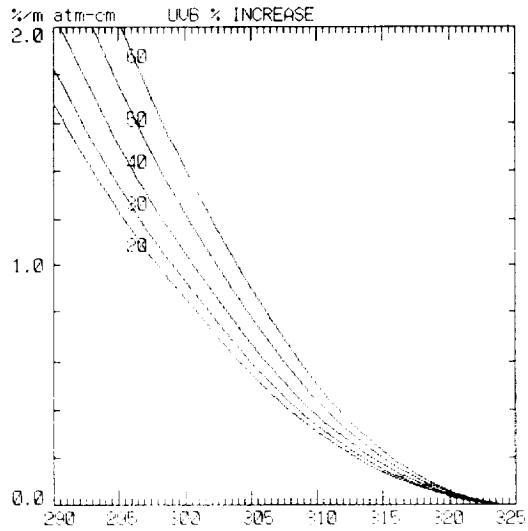

Fig. 6 Percent increase of the monochromatic UV irradiance due to 1 m atm-cm decrease of total ozone for the indicated solar zenith angles indicated by the number attached to the curves.

where λ_{av} is a kind of weighted mean wavelength.

An assessment of DUV increase due to ozone depletion for any geographical location and any season can be made using Eqs. 6, 7 and 8, provided that the relevant ozone amount and solar zenith angle are given. Some results are shown in Fig. 7 and in Tables 2 and 3.

Table 2 shows the monthly DUV-RAC in Tsukuba. The table also contains the widely used parameter, DUV-RAF (Radiation Amplification Factor) indicating the percent change of DUV due to a 1% change of total ozone. DUV-RAC is computed using the monthly average of total ozone and the solar zenith angle at noon on the fifteenth day of the month. DUV-RAF is obtained by multiplying DUV-RAC together with 1% of the monthly average of total ozone. The calculated DUV-RAC has the value of 0.60 ± 0.08 %/m atm-cm, with the minimum in April and May, and the maximum in November. DUV-RAF is correspondingly given by 1.85 ± 0.2 %/%. Roughly speaking, a 10% depletion of total ozone in the future will result in a 19% increase of UV irradiance at noon throughout the year, in middle latitudes.

Figure 7 includes the Northern Hemispheric distributions of total ozone, DUV-RAC and DUV-RAF. The ozone distribution is drawn on the basis of the 11 year averages of TOMS grid data (ver. 5) corrected by Japanese Dobson values. The value of DUV-RAC is computed each grid with the total ozone at the grid point and the corresponding solar zenith angle at noon of the summer solstice (the values in the region between 25°N and 35°N are extrapolated). The value of DUV-RAF is computed each grid by multiplying RAC by 1% of the total ozone. In Fig. 7, it can be seen that the longitudinal variation in RAC (and also RAF) is less remarkable compared to the latitudinal variation.

Table 3 shows the longitudinal averages of the grid data shown in Fig. 7. The value of DUV-RAC marks the minimum between 45°N and 50°N, and the maximum at the equator and at latitudes between 75°N and 80°N. On the average, DUV-RAC ranges within 0.555 ± 0.035 %/m atm-cm, and DUV-RAF within 1.81 ± 0.28 %/%. It can be concluded

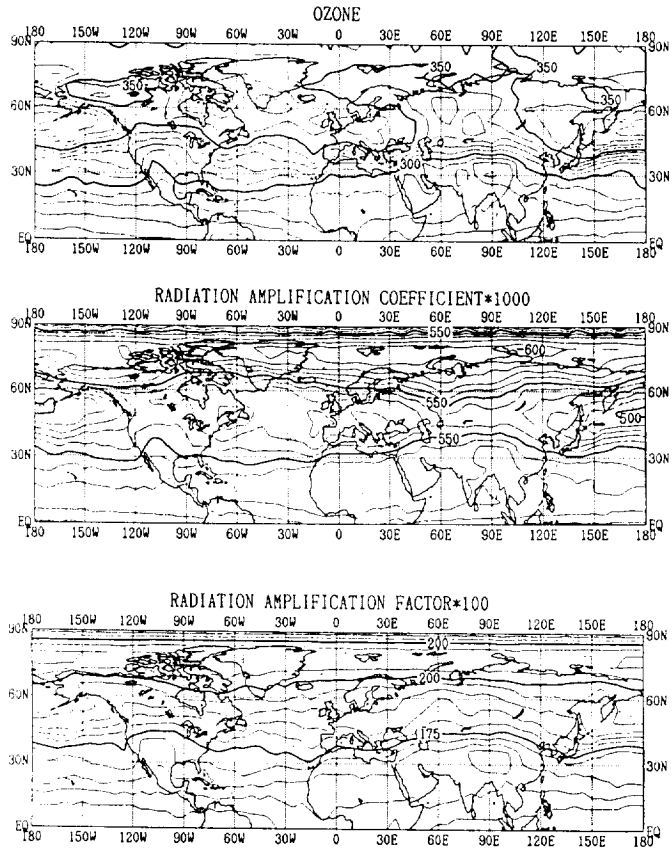

Fig. 7 Northern hemispheric distribution of total ozone (top), the radiation amplification coefficient (middle; multiplied by 1000) and the radiation amplification factor (bottom; multiplied by 100) at noon in mid-summer.

Tab. 2 Radiation amplification coefficients (RAC) and radiation amplification factors (RAF) of damaging ultraviolet (DUV) for noon in the northern mid-latitudes each month (MON).

MON	ZA	OZ	RAC	RAF
1	57.2	331	0.62	2.05
2	48.8	351	0.58	2.05
3	38.2	362	0.54	1.95
4	26.3	354	0.52	1.86
5	17.2	349	0.52	1.82
6	12.8	337	0.53	1.78
7	14.5	313	0.54	1.70
8	22.0	294	0.56	1.65
9	33.0	287	0.59	1.70
10	44.5	280	0.64	1.80
11	54.5	282	0.68	1.92
12	59.3	307	0.65	1.98

Tab. 3 Radiation amplification coefficients (RAC) and radiation amplification factors (RAF) of damaging ultraviolet (DUV) at noon in mid-summer of each latitude (LAT) of the Northern Hemisphere.

LAT	ZA	OZ	RAC	RAF
0	23.3	261	0.59	1.53
5	18.3	268	0.58	1.54
10	13.3	275	0.57	1.57
15	8.3	281	0.57	1.60
20	3.3	288	0.57	1.63
25	1.7	295	0.56	1.66
30	6.7	302	0.56	1.67
35	11.7	313	0.55	1.70
40	16.7	331	0.53	1.76
45	21.7	351	0.52	1.83
50	26.7	361	0.52	1.88
55	31.7	363	0.53	1.91
60	36.7	359	0.54	1.94
65	41.7	353	0.56	1.97
70	46.7	353	0.57	2.03
75	51.7	356	0.59	2.08
80	56.7	353	0.59	2.09
85	61.7	355	0.57	2.02

from Table 3 that DUV at noon on the summer solstice would increase by about 5.6% due to the ozone depletion of 10 m atm-cm throughout the Northern Hemisphere.

The present method to evaluate RAF or RAC for DUV can be similarly utilized for other action spectra. It may also be used for assessing the geographical distribution of UV increase due to the predicted geographical distribution of ozone depletion.

4. SUMMARY

The procedure estimating the UV increase due to ozone depletion is described, based on the simultaneous observation of spectral global UV irradiance with the Brewer and the total ozone with the Dobson. Noting the similarity in shapes among observed spectra, the reference UV spectrum is determined as a function of solar zenith angle, based on the observed data, which give a practical maximum of spectral irradiance for a given solar zenith angle. An observed spectrum is expressed by a simple combination of the reference spectrum and two parameters expressing the deformation of the observed spectrum from the reference. The percent increase of monochromatic UV irradiance due to the ozone depletion of 1 m atm-cm is evaluated by using the regression coefficient between the deformation parameter and total ozone, determined as a function of solar zenith angle. Also, the seasonal and geographical distribution of the percent change of DUV due to ozone depletion is evaluated.

The results show the DUV irradiance increases about 19% with the ozone depletion of 10% at noon throughout the year in the northern midlatitudes. Furthermore, the DUV at noon on the summer solstice increases about 5.6% with the ozone depletion of 10 m atm-cm for all latitudes in the Northern Hemisphere.

REFERENCES

Cutchis, P., 1974: Stratospheric ozone depletion and solar ultraviolet radiation on the earth. Science, 184, 13-19.

Dave, J. V. and P. Halpern, 1976: Effect of changes in ozone amount on the ultraviolet radiation received at sea level of a model atmosphere. Atmospheric Environment, 10, 547-555.

Gelstl, S. A. W., A. Zardecki, and H. L. Wiser, 1981: Biologically damaging radiation amplified by ozone depletions. Nature, 294, 352-354.

Ito, T., T. Ueno, R. Kajihara, M. Shitamichi, T. Uekubo, M. Ito, and M. Kobayashi, 1991: Development of monitoring technique of ultraviolet irradiance on the ground - an assessment of UV-B increase due to ozone depletion based on spectral observations. J. Meteor. Res, 43, 213-273.

Josefsson, W., 1986: Solar ultraviolet radiation in Sweden. SMHI Reports Meteorology and Climatology, RMK53, 77pp.

Pyle, J. A., and R. G. Derwent, 1980: Possible ozone reductions and UV changes at the earth's surface. Nature, 286, 373-375.

Venkateswaran, S. V., 1974: Solar ultraviolet radiation reaching the earth's surface. Proc. third conference on CIAP, 428-436.

Wester, U., 1981: A simple formulae approximation of the ACGIH curve of relative effectiveness of actinic UV. RI Internal Report, Dept. of Radiation Physics, Karolinska Institute, S-1041 Stokholm, 15pp.